Engineering Solid Mechanics 12 (2024) 65-80

Contents lists available at GrowingScience

Engineering Solid Mechanics

homepage: www.GrowingScience.com/esm

Elastic properties evaluation of banana-hemp fiber-based hybrid composite with nano-titanium oxide filler: Analytical and Simulation Study

Tanvi Saxena[a] and V.K. Chawla[a*]

[a]*Department of Mechanical and Automation Engineering, Indira Gandhi Delhi Technical University for Women, India*

ARTICLE INFO

Article history:
Received 10 March 2023
Accepted 4 July 2023
Available online
4 July 2023

Keywords:
Banana fiber
Elastic properties
Hemp fiber
Hybrid composite
Nano-titanium oxide filler

ABSTRACT

In recent years, nano-filler-based hybrid composites have gained significant attention from the research community; The nano-filler-based hybrid composites can have potential applications in numerous sectors. Nano-fillers are bringing a leading development in material science and natural fibers-based composites. The present study considers the impact of various weight percentages of nano-titanium oxide ($NTiO_2$) fillers (2%, 4%, and 6%) on the elastic features of novel hybridized banana-hemp fiber-reinforced epoxy composites. The proposed composite is analyzed for its elastic properties like longitudinal and transverse elastic modulus, axial Poisson's ratio, and axial shear modulus using homogenized micromechanical models, namely, Mori-Tanaka (M-T) model, Generalized self-consistent (G-SC) model and Modified Halpin-Tsai (M-HTS) model. The composite is modeled using one layer of banana fiber, one layer of $NTiO_2$ and epoxy, and one layer of hemp fiber. All three layers of the composite are arranged in the sequence of banana fiber at 45^0, a layer of $NTiO_2$ and epoxy at $0^{0,}$ and hemp fiber at 45^0. The proposed composite's vector sum deformation and strength are examined by employing the ANSYS APDL application. The results obtained in this study are compared with the experimental work mentioned in the literature. The composite reinforced with six weight% $NTiO_2$ has the highest mechanical strength, and the modified Halpin-Tsai (M-HTS) model is the most effective in calculating the elastic features of the proposed composite. In addition to the above, the hybridization effect for the proposed composite is also estimated to analyze the tensile failure strain of banana and hemp fiber in the proposed hybrid composite structure.

Abbreviations

$V_{fib/max/NTiO_2}$	The volume fraction of fiber, matrix, and nano-titanium oxide.
$W_{fib/max/NTiO_2}$	Weight% of fiber, matrix, and nano-titanium oxide.
$\rho_{fib/max/NTiO_2}$	The density of fiber, matrix, and nano-titanium oxide.
ρ_{CO}	The density of the composite.
$W_{BAF}/W_{HEF}/W_{EPO}/W_{NTiO_2}$	Weight% of banana fiber, hemp fiber, epoxy, and nano-titanium oxide.
$\rho_{BAF}/\rho_{HEF}/\rho_{EPO}/\rho_{NTiO2}$	Density of banana fiber, hemp fiber, epoxy, and nano-titanium oxide.
$V_{BAF}/V_{HEF}/V_{EPO}/V_{NTiO_2}$	Volume fraction of banana fiber, hemp fiber, epoxy, and nano-titanium oxide.
E^{LO}	Longitudinal elastic modulus of the composite.
E^{TRA}	Transverse elastic modulus of the composite.
$E_1^{fib/max}$	Longitudinal elastic modulus of fiber and matrix.

* Corresponding author.
E-mail addresses: vivekchawla@igdtuw.ac.in (V.K. Chawla)

ISSN 2291-8752 (Online) - ISSN 2291-8744 (Print)

doi: 10.5267/j.esm.2023.7.001

$E_{22}^{fib} = E_{33}^{fib}$	Transverse elastic modulus of fiber.
$G_{12}^{fib/max} = G_{13}^{fib/max}$	In-plane shear modulus of fiber and matrix.
G_{23}^{fib}	Out-of-plane shear modulus of fiber.
$\upsilon_{12}^{fib/max} = \upsilon_{31}^{fib/max}$	In-plane Poisson's ratio of fiber and matrix.
υ_{23}^{fib}	Out-of-plane Poisson's ratio of fiber
$\rho^{fib/max}$	The density of fiber and matrix.
$K_{23}^{\max} / K_{23}^{fib}$	Bulk modulus of fiber and matrix.
ξ'_{E_2}	
η'_{E_2}	
$\xi'_{G_{12}}$	Immeasurable parameters.
$\eta'_{G_{12}}$	
υ_{AX}	Axial Poisson's Ratio
G_{AX}	Axial Shear Modulus
$E_{1,ENTiO_2} = E_{3,ENTiO_2}$	Elastic modulus of nano-titanium oxide in an axial direction.
$E_{2,ENTiO_2}$	Elastic modulus of nano-titanium oxide in the transverse direction.
$G_{12,ENTiO_2} = G_{32,ENTiO_2}$	In-plane shear modulus of nano-titanium oxide.
$\upsilon_{12,ENTiO_2} = \upsilon_{32,ENTiO_2}$	In-plane Poisson's ratio of nano-titanium oxide.
$\upsilon_{13,ENTiO_2}$	Out-of-plane Poisson's ratio of nano-titanium oxide.

1. Introduction

Natural fiber blended green hybrid composites are being immensely utilized nowadays because of their tremendous features like renewability, biodegradability, low weight, and environmental aspects (Pol et al., 2022; Sadjadi, 2021; Tekletsadik, 2023). Banana fiber is a leaf fiber, and hemp fiber is a bast fiber. Both are natural fibers and find countless applications in the automobile and aerospace sectors. As mentioned above, the fibers are readily available, highly rigid, and have fire-defiant characteristics. Among natural fibers, banana fiber is found to be sustainable for increasing the mechanical properties of resins (Saxena & Chawla, 2021, 2022a). For sustainable development, green technologies are gaining the attention of researchers globally (Singh & Angra, 2018; Gupta et al., 2022; Chawla et al., 2021a; Chawla et al., 2023; Sadjadi & Ghaderi, 2023). Polymer matrix reinforced natural fiber composites have magnificent mechanical and chemical features like high strength and modulus, superior fatigue, corrosion, and abrasion resistance (Saxena & Chawla, 2022b; Parashar & Chawla, 2023). These composites are suitable alternatives to aircraft, warships, buildings, and electrical and electronic items in numerous applications. Sapaun et al. (2006) fabricated three composite samples using banana fiber. The authors prepared the samples for their proposed composite with different configurations, and maximum stress, Young's modulus, and maximum deformation under various load conditions are evaluated (Sapaun et al., 2006). Hemp fiber has commendable binding characteristics, improving tensile strength and stiffness in acrid surroundings (Wang, 2002; Wang et al., 2001; Parashar & Chawla, 2021, 2022). Kobyashi et al. (2014) studied the characteristics and manufacturing of hemp fiber-based goods composites using the micro braiding process. They discovered that hemp fiber could be a suitable binder for goods composites. Banana fiber-reinforced composites have better tensile features and less deviation than flax fiber-reinforced composites (Kobyashi et al., 2014). Also, banana and hemp fiber blended composites carry added bending and impact strength in contrast to hemp and glass fiber blended polymer composites (Li et al., 2006).

Different configurations of polymer matrix and nanoparticles have been studied in the last few years. The incorporation of small quantity of nano-filler has been found to significantly enhance the substantial properties of polymer matrices. The critical parameters that influence the characteristics of polymer blended composites are shape, size, content, and amount of agglomeration of the filler (Kumar et al., 2020a; Bhatia et al., 2021; Saxena et al., 2021). Nanoparticles also have distinctive characteristics like electrical, photonic, and magnetism which develop limitless possibilities for fast technological use (Yadav et al., 2022; Chawla et al., 2021b). Faghidian, (2021) proposed a modified theory of elasticity to provide a practical approach to the nanoscopic study of class variables. Particle polymer composites comprise nanoparticles of different varieties and shapes distributed randomly in matrix structures. The addition of nano-silicon dioxide increased mechanical properties and breakage resilience with increasing wt% due to the development of void deformations in the matrix, and delamination of particle-matrix (Mahesha et al., 2022). Titanium oxide (TiO_2) nanoparticles are gaining more popularity today (Raghvendra

et al., 2015; Perreault et al., 2015). They are becoming popular due to their peculiar characteristics and potential applications in perfumes and cosmetics (Mahesha et al., 2022). Polymer nanocomposites reinforced with TiO_2 nanoparticles and epoxy resin is processed ultrasonically, and mechanical and permeable features of the final composites are compared to the nanocomposites and the epoxy matrix, and the neat matrix (Seshanandan et al., 2016). It is found that nanocomposites containing TiO_2 nanoparticles at low weight% loading showed an increment in abrasion resistance in contrast to the neat matrix (Seshanandan et al., 2016).

The scholarly articles show that the composite material developed with banana fiber and hemp fiber blended with TiO_2 nanoparticles and epoxy resin had never been explored earlier for its elastic and mechanical properties. Additionally, the hybridization effect for the proposed composite has never been calculated before by any researcher. Therefore, to bridge the above-mentioned research gap, in this paper following research problems are addressed:

- A novel composite of banana and hemp fiber reinforced with different weight percentages of TiO_2 nanoparticle and epoxy resin bearing a transverse load of 250 KN (in -z-direction) is designed in ANSYS APDL.
- The elastic and mechanical features of the newly proposed composite are evaluated and analyzed using Mori-Tanaka, a generalized self-consistent model, and modified Halpin-Tsai models for different volume fractions of banana fiber, hemp fiber, TiO_2 nanoparticles, and epoxy matrix.
- The strength and deformation of the proposed composite blended with 2%, 4%, and 6% of $NTiO_2$ particles and 61%, 59%, and 57% of epoxy resin are analyzed at various orientation angles by using ANSYS APDL application
- The hybridization effect for the composite is also calculated to examine the tensile failure strain characteristics of banana and hemp fiber in the proposed hybrid composite material.
- The tensile and shear stress results for the proposed composite obtained from simulation results are compared with the experimental results (Mahesha et al., 2022).

In this paper, Mori-Tanaka (M-T), generalized self-consistent model, and modified Halpin-Tsai models (Mod. H-T) are used to examine the impact of incorporating the TiO_2 nanoparticles on the elastic features of the banana fiber and hemp fiber blended with epoxy composites. Besides efficiency and mechanical equations for the elastic features, the principal benefit of this paper is the hybridization effect and incorporation of different weight percentages of TiO_2 nanoparticles at different orientations of fibers. The prediction of the elastic properties is justified by validating it with the laboratory results provided in the literature. Additionally, the impact of the volume fraction of banana and hemp fibers with varying wt. % of TiO_2 nanoparticles and epoxy resin on the elastic properties are also examined.

2. Modeling of Proposed Bio-Composite

In this section, the layers of banana fiber, hemp fiber, and layers of TiO_2 nanoparticles dispersed in the epoxy resin are arranged to form a composite sandwich structure. The average particle size of nano TiO_2 is 50 nm (Seshanandan et al., 2016). If nanoparticles have an anisotropic configuration, their direction should be considered in determining the material properties (Yung et al., 2006; Saxena & Tomar, 2019; Parashar & Tomar, 2019). The proposed composite is designed using semi-empirical and homogenization models by changing the weight percentage of TiO_2 nanoparticles and epoxy resin while the percent weight of banana fiber and hemp fiber is kept fixed, as given in Table 1.

Table 1. Weight percentages of fibers, matrix, and nano-TiO_2 (Mahesha et al., 2022).

Sequence	Banana fiber (%)	Hemp fiber (%)	Epoxy (%)	Nano-TiO_2 (%)
I	7	30	61	2
II	7	30	59	4
III	7	30	57	6

The elastic features of banana fiber, hemp fiber, epoxy, and nano-TiO_2 are shown in Table 2.

Table 2. Elastic features of banana, hemp fiber, epoxy resin, and $NTiO_2$

Features	*Banana fiber (Dixit & Padhee, 2019)*	*Hemp fiber (Seshanandan, 2016)*	*Epoxy (Dixit & Padhee, 2019)*	*Nano-TiO_2 (Seshanandan, 2016)*
$E_1^{fib/max}$ *(GPa)*	*3.48*	*70*	*35*	$E_{NTiO_2} = 244$
$E_{22}^{fib} = E_{33}^{fib}$ *(GPa)*	---	---	---	---
$G_{12}^{fib/max} = G_{13}^{fib/max}$ *(GPa)*	*4*	*4*	*0.32*	$G_{NTiO_2} = 95$
G_{23}^{fib} *(GPa)*	---	---	---	---
$\upsilon_{12}^{fib/max} = \upsilon_{31}^{fib/max}$	*0.28*	*0.36*	*0.35*	$\upsilon_{NTiO_2} = 0.27$
υ_{23}^{fib}	---	---	---	---
$\rho^{fib/max}$ *(kg/m³)*	*1350*	*860*	*1270*	*4230*

The fibers, matrix, and filler volume fractions are evaluated using the following equations (DeArmitt, 2011) and are given in Table 3.

Table 3. Evaluated volume fractions of fibers, matrix, and nano-TiO_2

Sequence	Banana fiber (BAF)	Hemp fiber (HEF)	Epoxy	Nano-TiO_2 ($NTiO_2$)
	V_{BAF}	V_{HEF}	V_{EPO}	V_{NTiO_2}
A	0.06	0.39	0.54	5.834×10^{-3}
B	0.06	0.39	0.53	0.01
C	0.06	0.4	0.52	0.02

where

$$V_{fib/max/NTO} = \frac{W_{fib/max/NTiO_2}}{\rho_{fib/max/NTiO_2}} \times \rho_{CO} \tag{1}$$

$$\rho_{CO} = \frac{1}{\frac{W_{BAF}}{\rho_{BAF}} + \frac{W_{HEF}}{\rho_{HEF}} + \frac{W_{EPO}}{\rho_{EPO}} + \frac{W_{NTiO_2}}{\rho_{NTiO_2}}} \tag{2}$$

3. Homogenized Models

Homogenized models are based on analytical equations to calculate the constituent features of the composite structure, such as the constituent's composition, properties, shape, volume fraction, inclination, etc. These properties depend on the comprehensive mechanical performance of the composite model. The homogenization models aim to determine the stress-strain behavior at the microscopic and macroscopic levels (Wang & Huang, 2017; Younes et al., 2012).

3.1. Mori-Tanaka Model

Micromechanical models such as Mori-Tanaka (M-TA) (Mori & Tanaka, 1973; Benveniste, 1987; Hill, 1965) and generalized self-consistent (Hill, 1965) have been utilized in computing different properties of short fiber composites. The M-TA model is used for composites made from short fiber and has yielded the best values for fillers with a large aspect ratio. This model employs Eshelby's inclusion theory. This model aims to envisage the general nature of fibers and matrces. The prime benefit of the M-TA model is that in the estimation of elastic features of nano-filler-based composite, it also considers the consequence of the shape and dimensions of the nanoparticles. To examine the mechanical characteristics of nanocomposites, various researchers have applied analytical models and simulation models (Seretis et al., 2017; Ojha et al., 2019; Hadden et al., 2015; Rafiee et al., 2018; Aliha et al., 2012, 2015). The longitudinal and transverse Young's modulus, axial Poisson's ratio, and axial shear modulus are given by the following equations (Abaimov et al., 2016):

$$E_{LO} = V_{fib}E_1^{fib} + (1-V_{fib})E^{max} + 2V_{fib}(1-V_{fib})Z_1(\upsilon_{12}^{fib} - \upsilon^{max})^2 \tag{3}$$

$$E_{TRA} = \frac{E_1}{[1-(\upsilon^{max})^2](Y_1+Y_2)} \tag{4}$$

$$\upsilon_{AX} = \upsilon^{max} + 2V_{fib}\frac{Z_1}{E^{max}}(\upsilon_{12}^{fib} - \upsilon^{max})[1-(\upsilon^{max})^2] \tag{5}$$

$$G_{AX} = \frac{E^{max}}{2(1-V_{fib})(1+\upsilon^{max})}\left[1+V_{fib} - \frac{4V_{fib}}{1+V_{fib}+2(1-V_{fib})\frac{G_{12}^{fib}}{E^{max}}(1+\upsilon^{max})}\right] \tag{6}$$

$$Y_1 = V_{fib}Z_1\left(\frac{E_1^{fib}}{E^{max}}\right)\left[\frac{1+\upsilon^{max}}{E^{max}} - \frac{2}{E_1^{fib}} + \frac{1+\upsilon_{23}^{fib}}{E_2^{fib}}\right] \tag{7}$$

$$Y_2 = \frac{1}{1-(\upsilon^{max})} + 2V_{fib}\left(\frac{E_1}{Z_2}\right)\left[1+\upsilon_{23}^{fib} - \frac{E_2^{fib}}{E^{max}}(1-\upsilon^{max})\right] \tag{8}$$

$$Z_1 = \left\{ -2(1-V_{fib})\frac{(\upsilon_{23}{}^{fib})^2}{E_1{}^{fib}} + (1-V_{fib})\frac{1-\upsilon_{23}{}^{fib}}{E_2{}^{fib}} + \frac{(1+\upsilon^{max})[1+V_{fib}(1-2\upsilon^{max})}{E^{max}} \right\} \tag{9}$$

$$Z_2 = E_2{}^{fib}(3+V_{fib}-4\upsilon^{max})(1+\upsilon^{max}) + (1-V_{fb})E^{max}(1+\upsilon_{23}{}^{fib}) \tag{10}$$

For 2% $NTiO_2$, the elastic features of banana-hemp fiber-blended $NTiO_2$ particles an epoxy composite can be evaluated using Eqs.(3) - (6):

$$E_{LO} = 46.4GPa + E_{1,EPO+NTiO_2} = 46.4 + 20.2 = 66.6GPa$$

where: $Z_{1_{BAF}} = 25.46; Z_{1_{HAF}} = 23.21; Z_{1_{NTiO_2}} = 25.89;$ (Values calculated using Eq. (9))

$$E_{TRA} = 13.12GPa + E_{2,EPO+NTiO_2} = 13.12 + 65.1 = 78.2GPa$$
$$\upsilon_{AX} = 0.4 + \upsilon_{12,EPO+NTiO_2} = 0.14 + 0.10 = 0.24$$
$$G_{AX} = 26.87GPa + G_{12,EPO+NTiO_2} = 26.87 + 7.5 = 34.4GPa$$

where: $Y_{1_{BAF}} = 0.08; Y_{2_{BAF}} = 1.15; Y_{1_{HAF}} = 0.18; Y_{2_{HAF}} = 3.7; Z_{2_{HAF}} = 21.35$ (Values calculated using Eq. (7), (8), and (10))

Similarly, the elastic properties of the proposed composite are evaluated for 4% and 6% $NTiO_2$ and are given in Table 4.

3.2. Generalized Self-Consistent Model

The generalized self-consistent (GS-C) model was initially developed by (Hill, 1965; Budiansky, 1965) to calculate the elastic features of isotropic spherical particle-reinforced composite structures. This model determines the elastic features of short-fiber composites (Chou et al., 1980; Kumar et el., 2020b). In this model, a particulate consisting of elastic properties of short fiber is required to be placed in a uniform homogenous medium, where the neighboring medium has the undetermined elastic features of the composite that needs to be determined. The longitudinal Young's modulus, axial Poisson's ratio, and axial shear modulus are given by the following equations (Abaimov et al., 2016):

$$E_{LO} = E_1{}^{fib}V_{fib} + E^{max}(1-V_{fib}) + \frac{4V_{fib}(1-V_{fib})(\upsilon_{12}{}^{fib}-\upsilon^{max})^2}{\frac{(1-V_{fib})}{K_{23}{}^{fib}} + \frac{V_{fib}}{K_{23}{}^{max}} + \frac{1}{G^{max}}} \tag{11}$$

$$\upsilon_{AX} = \upsilon_{12}{}^{fib}V_{fib} + \upsilon^{max}(1-V_{fib}) + \frac{V_{fib}(1-V_{fib})(\upsilon_{12}{}^{fib}-\upsilon^{max})\left(\frac{1}{K_{23}{}^{max}} - \frac{1}{K_{23}{}^{fib}}\right)}{\frac{(1-V_{fib})}{K_{23}{}^{fib}} + \frac{V_{fib}}{K_{23}{}^{max}} + \frac{1}{G^{max}}} \tag{12}$$

$$G_{AX} = G^{max}\frac{G_{12}{}^{fib}(1+V_{fib}) + G^{max}(1-V_{fib})}{G_{12}{}^{fib}(1-V_{fib}) + G^{max}(1+V_{fib})} \tag{13}$$

For 2% $NTiO_2$, the elastic features of banana-hemp fiber-blended NTiO2 particles and epoxy composite can be evaluated using Eqs. (11) - (13):

$$E_{LO} = 66.6GPa$$

$$\upsilon_{AX} = 0.14 + \upsilon_{12,EPO+NTiO_2} = 0.14 + 0.10 = 0.24 \quad G_{AX} = 27.3GPa + G_{12,EPO+NTiO_2} = 27.3 + 7.5 = 34.8GPa$$

Similarly, elastic features of the proposed composite are evaluated for 4% and 6% $NTiO_2$ and are given in Table 4.

3.3. Modified Halpin-Tsai Model

The modified Halpin-Tsai model (M-HTS) is a semi-empirical micromechanical model formed by Halpin-Tsai to improve the transverse elastic modulus as attained by the rule of mixture. The M-HTS model, also known as a semi-physical model, is based on parameters having natural importance (Dahlen & Springer, 1994; Ramakrishna et al., 2006). Semi-empirical relations have fitting parameters that make modeling simple and easy (Genin & Birman, 2009; Alvinasab, 2009). The M-HTS model evaluates the matrix modulus for fiber diameter by exhibiting an equivalent constant. The M-HTS method relies on finite element research, considering the prospects of multiple fiber configurations (Giner et al., 2015). The transverse Young's modulus and axial shear modulus as suggested by (Halpin, 1969), are given by:

$$E_{TRA} = E^{max}\left(\frac{1+\xi'_{E_2}\eta'_{E_2}V^{BAF/HEF}}{1-\xi'_{E_2}V^{BAF/HEF}}\right) \tag{14}$$

$$G_{AX} = G^{max}\left(\frac{1+\xi'_{G_{12}}\eta'_{G_{12}}V^{BAF/HEF}}{1-\eta G_{12}V^{BAF/HEF}}\right) \tag{15}$$

where, $V^{BAF}, V^{HEF} < 0.3$

$$\eta_{E_2} = \frac{\left(\frac{E_2^{BAF/HAF}}{E^{max}}\right)-1}{\left(\frac{E_2^{BAF/HAF}}{E^{max}}\right)+\xi_{E_2}} \tag{16}$$

where:

$$\xi_{E_2} = \begin{cases} 4.924 - 35.888V^{BAF/HEF} + 125.118V^{BAF^2/HEF^2} - 145.121V^{BAF^3/HEF^3} & \text{if} \quad V^{BAF}, V^{HAF} < 0.3 \\ 1.5 + 5500V^{BAF^{18}/HEF^{18}} & \text{if} \quad V^{BAF}, V^{HAF} \geq 0.3 \end{cases}$$

$$\eta_{G_{12}} = \frac{\left(\frac{G_{12}^{BAF/HEF}}{G^{max}}\right)-1}{\left(\frac{G_{12}^{BAF}}{G^{max}}\right)+\xi_{G_{12}}}; \xi_{G_{12}} = 1 + 40V^{BAF^{10}/HEF^{10}} \tag{17}$$

The following equations of longitudinal elastic modulus and axial Poisson's ratio are given by (Dahlen & Springer, 1994).

$$E_{LO} = E_1^{BAF}V^{BAF} + E_1^{HEF}V^{HEF} + E_{1,EPO+NTiO_2} \tag{18}$$

$$\upsilon_{AX} = \upsilon_{12}^{BAF}V^{BAF} + \upsilon_{12}^{HEF}V^{HEF} + \upsilon_{12,EPO+NTiO_2} \tag{19}$$

For 2% $NTiO_2$, the elastic features of banana-hemp fiber-blended NTiO2 particles and epoxy composite can be evaluated using eqs. (14) - (19):

$$E_{LO} = 66.6GPa \quad G_{AX} = 27.5GPa + G_{12,EPO+NTiO_2} = 27.5 + 7.5 = 35.0GPa \quad \upsilon_{AX} = 0.35 + \upsilon_{12,EPO+NTiO_2} = 0.15 + 0.10 = 0.25$$

Similarly, elastic features of the proposed composite are evaluated for 4% and 6% nano-TiO_2 and are given in Table 4.

3.4. Calculation of elastic properties for nano-TiO_2 with epoxy resin

$NTiO_2$ particles with different weight percentages (2%, 4%, 6%) are mixed with epoxy resin and are used as a binding medium in modeling the proposed composite. The formulae below are as per modified ROM for calculating the elastic properties of nano-TiO_2 with epoxy resin (Tsai & Hahn, 2018).

$$E_{1,ENTiO_2} = E_{3,ENTiO_2} = V_{max}E_{max} + V_{NTiO_2}E_{NTiO_2} \tag{20}$$

$$E_{2,ENTiO_2} = \frac{E_{max} E_{NTiO_2}}{V_{max} E_{NTiO_2} + V_{NTiO_2} E_{max} - V_{max} V_{NTiO_2} \beta E_{max} E_{NTiO_2}} \tag{21}$$

$$\upsilon_{13,ENTiO_2} = \frac{V_{max} \upsilon_{max} E_{max} (1 - \upsilon_{NTiO_2}{}^2) + V_{NTiO_2} \upsilon_{NTiO_2} E_{NTiO_2} (1 - \upsilon_{max}{}^2)}{V_{max} E_{max} (1 - \upsilon_{NTiO_2}{}^2) + V_{NTiO_2} \upsilon_{NTiO_2} E_{NTiO_2} (1 - \upsilon_{max}{}^2)} \tag{22}$$

$$\upsilon_{12,ENTiO_2} = \upsilon_{32,ENTiO_2} = V_{max} \upsilon_{NTiO_2} + V_{NTiO_2} \upsilon_{max} \tag{23}$$

$$G_{12,ENTiO_2} = G_{32,ENTiO_2} = \frac{G_{NTiO_2} G_{max}}{V_{max} G_{NTiO_2} + V_{NTiO_2} G_{max} - V_{max} V_{NTiO_2} \eta G_{max} G_{NTiO_2}} \tag{24}$$

$$G_{12,ENTiO_2} = \frac{E_{1,ENTiO_2}}{2(1 + \upsilon_{13,ENTiO_2})} \tag{25}$$

where:

$$\beta = \frac{\upsilon_{max}{}^2 \frac{E_{NTiO_2}}{E_{max}} + \upsilon_{NTiO_2}{}^2 \frac{E_{max}}{E_{NTiO_2}} - 2\upsilon_{max} \upsilon_{NTiO_2}}{V_{max} E_{max} + V_{NTiO_2} E_{NTiO_2}} \tag{26}$$

$$\eta = \frac{\upsilon_{max}{}^2 \frac{G_{NTiO_2}}{G_{max}} + \upsilon_{NTiO_2}{}^2 \frac{G_{max}}{G_{NTiO_2}} - -2\upsilon_{max} \upsilon_{NTiO_2}}{V_{max} G_{max} + V_{NTiO_2} G_{max}} \tag{27}$$

For 2% Nano-TiO_2, $E_{1,ENTiO_2} = 20.2GPa$, $E_{2,ENTiO_2} = 65.1GPa$, $\upsilon_{12,ENTiO_2} = 0.10$,

$G_{12,ENTiO_2} = G_{32,ENTiO_2} = 7.5GPa$, where: $\beta = 0.03$, $\eta = 53.2$

4. Fiber hybridization and its utilization

Fiber hybridization enhances and examines the composite features (Essabir et al., 2016; Thwe & Liao, 2002). Fiber hybridization is significant in deciding the nature of fibers in the hybrid composite. It determines the tensile strain at which hybrid composite fails and how this strain varies with the failure strain of the composite reinforced with a single fiber. Hybrid composites are made up of high-elastic and low-elastic fibers. The fibers that resist breakage are called high-elastic fibers, and fibers that tend to break easily are called low-elastic fibers. In the current study, high elastic fiber is hemp, and low elastic fiber is banana.

The hybrid effect R_{hbr}, as given by (Zweben, 1977), is:

$$R_{hbr} = \left[\frac{\gamma_h (m_h{}^q - 1)}{2\gamma (m^s - 1)} \right]^{\frac{-1}{2s}} \tag{28}$$

The unproductive length γ and γ_h for the hybrid composite is given by (Zweben, 1977):

$$\gamma = 1.531 \left(\frac{E_1 A_1{}' s}{H h_e} \right)^{1/2} \tag{29}$$

$$\gamma_h = \frac{2}{\rho'^{1/2}} \left(\frac{E_1 A'_1 s}{H h_e} \right)^{1/2} \frac{n'_2{}^2 - n'_1{}^2}{n'_1 (2 - n'_1{}^2) - n'_2 (2 - n'_2{}^2)} \tag{30}$$

where: the ratio of fibers' extensional stiffness (ρ') is given by (Zweben, 1977):

$$\rho' = \frac{E_1 A_1'}{E_2 A_2'} \text{ and } \rho' = \frac{3.48}{70} = 0.05$$

where:

$E_1 A_1'$ = Exact stiffness of low elastic fibers (LEF) (banana fiber).

$E_2 A_2'$ = Exact stiffness of high elastic fibers (HEF) (hemp fiber).

h_e = Matrix height.

S = Distance between fibers.

H = Shear modulus of the matrix.

The strain and strain concentration factors K' and K_h' respectively, and a constant $n'_{1,2}$ are given by (Zweben, 1977):

$$n = 1.293$$

$$K_h^{'} = 1 + \frac{n_2^{'} - n_1^{'}}{n_1^{'}(2 - n_1^{'2}) - n_2^{'}(2 - n_2^{'2})} \tag{31}$$

$$m_{1,2}^{'} = \left(\frac{\rho^{'} + 1 \pm (\rho^{'2} + 1)^{1/2}}{\rho^{'}} \right)^{1/2} \tag{32}$$

Substituting the value $\rho^{'}$ obtained above in Eq. (32), we get:

$n_1^{'} = 6.4$ and $n_2^{'} = 1.0$.

Substituting the values $m_1^{'} \& m_2^{'}$ obtained above in Eq. (31), we get:

$$K_h^{'} = 1.02$$

$\gamma \& \gamma_h$ are calculated using Eqs. (29) and (30) as:

$$\gamma = 1.531 \left(\frac{3.48 \times (200 \times 30) \times 30}{0.32 \times 1 \times 1000^2} \right)^{1/2} = 2.1 \qquad \gamma_h = \frac{2}{\sqrt{0.05}} (3.6) \left(\frac{1.0^2 - 6.4^2}{6.4(2 - 6.4^2) - 1.0(2 - 1.0^2)} \right) = 1.9$$

$$\therefore R_{hbr} = \left[\frac{1.9(1.02^5 - 1)}{2 \times 2.1(1.293^5 - 1)} \right]^{-1/2 \times 5} ; s \approx 5$$

$$= \frac{0.19}{10.9} = 1.5$$

Therefore, the tensile strain at which banana-hemp fiber reinforced $NTiO_2$ and epoxy composite fails is 1.5 times higher than the composites made up of banana fibers alone.

5. Finite Element Model

5.1. Model Dimensions

The proposed composite specimen is modeled and analyzed for its mechanical features on ANSYS APDL application. The following assumptions are considered in this study:

- The composite has no irregularity and is free of voids.
- Fibers are aligned in the matrix uniformly.
- Fibers and matrix is affixed perfectly.
- The size of the fibers is the same.

The dimensions taken in this current study are according to ASTM D3039 grade (Dixit & Padhee, 2019): sample length= 30 mm, sample breadth = 200 mm, and lamina thickness = 1 mm/layer. The number of layers = 3 (Dixit & Padhee, 2019). Depth of each specimen = 3 mm, Boundary conditions: Degree of freedom = zero. The specimen sides are fully constrained. After modeling the sample, a mesh tool is used to mesh the sample. This study divides the specimen model into 20 meshes vertically and 15 meshes horizontally. Meshed model is shown in Fig. 1.

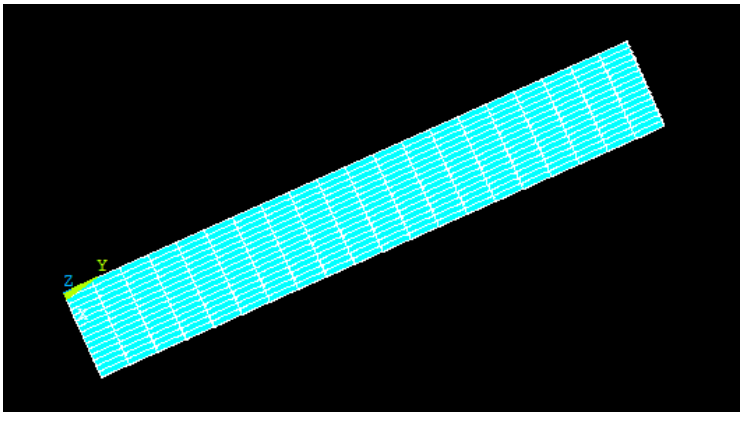

Fig. 1. Meshed model in ANSYS composite

5.2. Loads on the fibers and fibers orientation

The assessment of the properties is executed by using element 3D 4 Shell 181 (Dixit & Padhee, 2019). An application of 250 KN (Dixit & Padhee, 2019) point load is applied to the specimen at 21 nodes in the transverse direction (along -z-axis) as displayed in (Fig. 4). The specimen is laid in the order of layers: banana fiber - $NTiO_2$ and epoxy-hemp fiber at angles of 45^0, 0^0, 45^0 respectively also displayed in Fig. 2.

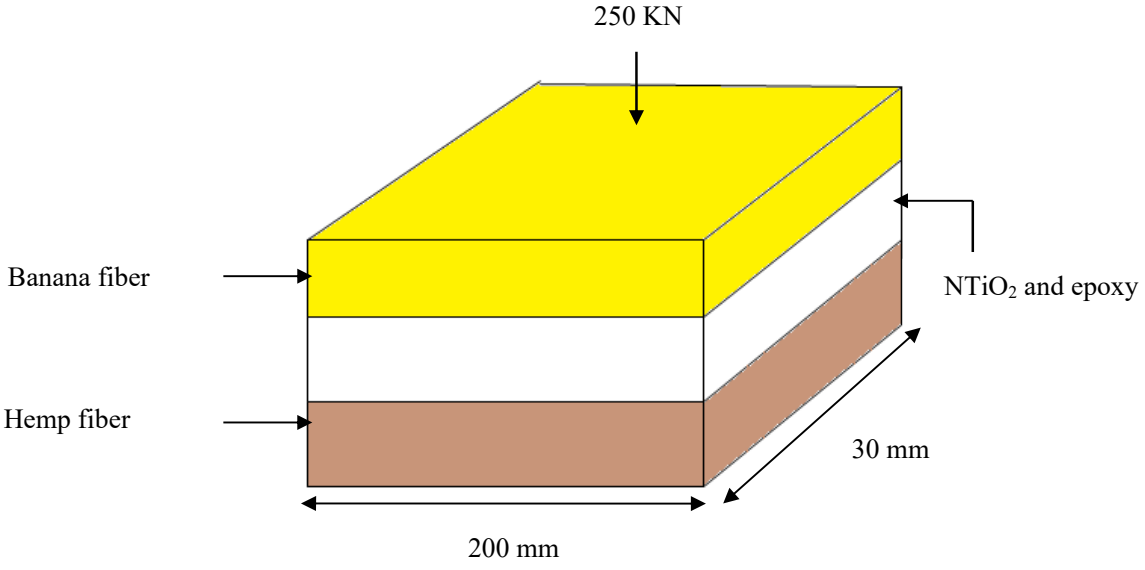

Fig. 2. Application of transverse point load on the proposed composite

The configuration of layers in ANSYS APDL is shown in Fig. 3. The total vector sum distortion for the proposed composite material reinforced with 2%, 4%, and 6% $NTiO_2$ particles is given in Table 4. The total vector sum distortion plots in ANSYS APDL application for $NTiO_2$composition of 2%, 4% & 6% are also shown in Fig. 5.

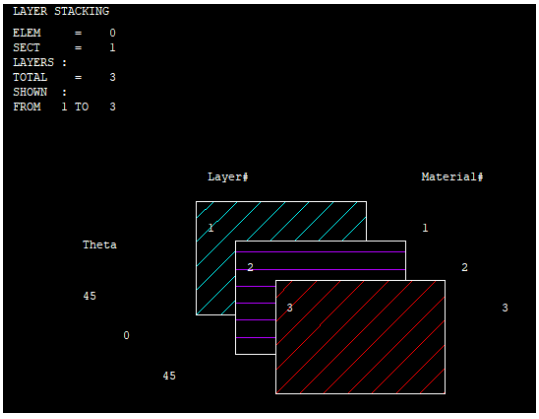

Fig. 3. Orientation of layers at 0^0 in ANSYS APDL

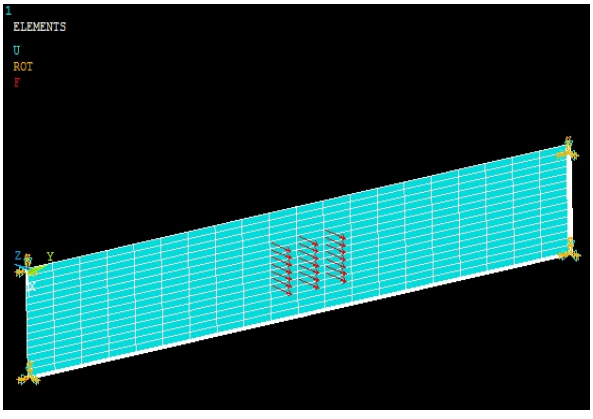

Fig. 4. Application of point load on the meshed model at 21 nodes

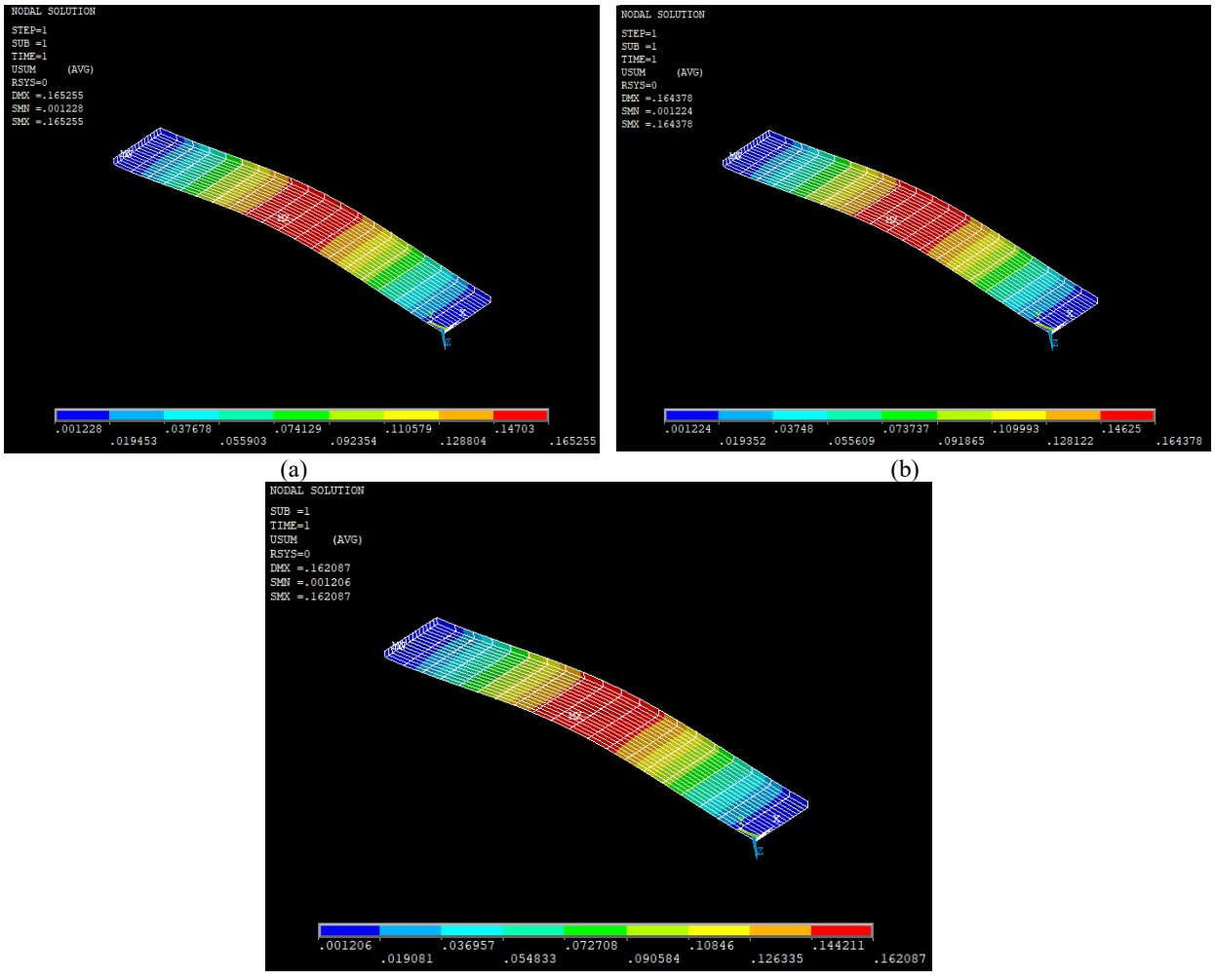

Fig. 5. Total vector sum distortion for banana-hemp fiber blended nano-titanium oxide ($NTiO_2$) and an epoxy resin having (a) 2 % (b) 4% (c) 6% $NTiO_2$

Table 4. Elastic properties, total vector sum distortion, and FEM results for different weight percentages of $NTiO_2$ reinforcement in the proposed composite

$NTiO_2$ %	Elastic Properties	Mori-Tanaka Model	Generalized Self-Consistent Model	Modified Halpin-Tsai Model	Total vector sum distortion from ANSYS	FE model
2%	E_1 (GPa)	66.6	66.6	66.6	0.16525 mm	68.2
	υ_{12}	0.24	0.24	0.25		0.26
	E_2 (GPa)	78.2	**	**		84.4
	G_{12} (GPa)	34.4	34.8	35.0		36.2
4%	E_1 (GPa)	68.2	67	67.1	0.16437 mm	69.1
	υ_{12}	0.48	0.48	0.48		0.49
	E_2 (GPa)	79.8	**	**		84.5
	G_{12} (GPa)	34.1	34.6	35.5		36.2
6%	E_1 (GPa)	70.2	69.5	69.5	0.16208 mm	71.3
	υ_{12}	0.49	0.49	0.48		0.50
	E_2 (GPa)	81.1	**	**		84.5
	G_{12} (GPa)	37.5	37.6	38.2		39.1

6. Results and Discussion

In the current study, the proposed composite material blended with 2%, 4% & 8% $NTiO_2$ particles is configured in ANSYS APDL. The main objective is to examine and compare elastic properties obtained from different analytical models and FEM simulations to determine the mean error and distortion for 2%, 4% & 6% $NTiO_2$ inclusions. The mean error (E_{ME}) is evaluated using the following equation (Loan & Gloub, 1996):

$$E_{ME} = \left| \frac{x_{any} - x_{fem}}{x_{fem}} \right| \times 100 \tag{33}$$

where: x_{any} = Values obtained by analytical models.

x_{fem} = Values obtained by finite element model.

Mahesha et al. (2022) conducted experiments to evaluate the tensile and shear stress of jute-hemp fiber reinforced nano titanium oxide hybrid-composite by varying the weight % of $NTiO_2$ filler. The composition of fibers and fillers used by Mahesha et al. (2022) and in this study are shown in Table 5. The results obtained for tensile and shear stress (Mahesha et al., 2022) are compared with the simulation results of the proposed composite, as shown in tabular form in Table 6. A decline of 61% in tensile stress and 55.6% in shear stress is observed in the proposed composite reinforced with 2 wt % $NTiO_2$ as compared to the value of tensile stress of 60 MPa and shear stress of 46 MPa for jute-hemp fibers reinforced with 2 wt % of $NTiO_2$ fillers (Mahesha et al., 2022). For 4 wt % of $NTiO_2$, the tensile stress shows a decline of 61.2% as compared to the value of tensile stress of 65 MPa, and shear stress shows a decline of 53.7% as compared to the value of shear stress of 53 MPa for jute-hemp fibers reinforced with 4 wt % of $NTiO_2$ fillers (Mahesha et al., 2022). Variation of tensile stress and shear stress for different weight percentages of $NTiO_2$ filler is given in Fig. 6.

Table 5. The weight percentage of fibers and filler used in this study and by (Mahesha et al., 2022).

S.No.	Fibers and filler Composition	Mahesha et al., (2022) (Experimental work) (wt%)	Proposed hybrid composite (wt%)
1	Hemp	30	30
2	$NTiO_2$	2	2
		4	4
		6	6
3	Epoxy	61	61
		59	59
		57	57
4	Banana	--	7
5	Jute	7	--

Table 6. A comparison of tensile and shear stress obtained by FEM for the proposed composite with the experimental results (Mahesha et al., 2022).

Nano-TiO_2 (%)	Mahesha et al., (2022)		Proposed Composite	
	Tensile stress (MPa)	Shear stress (MPa)	Tensile stress (MPa)	Shear stress (MPa)
2	60	46	23.4	20.4
4	65	53	25.2	24.5
6	68	57	28.0	26.7

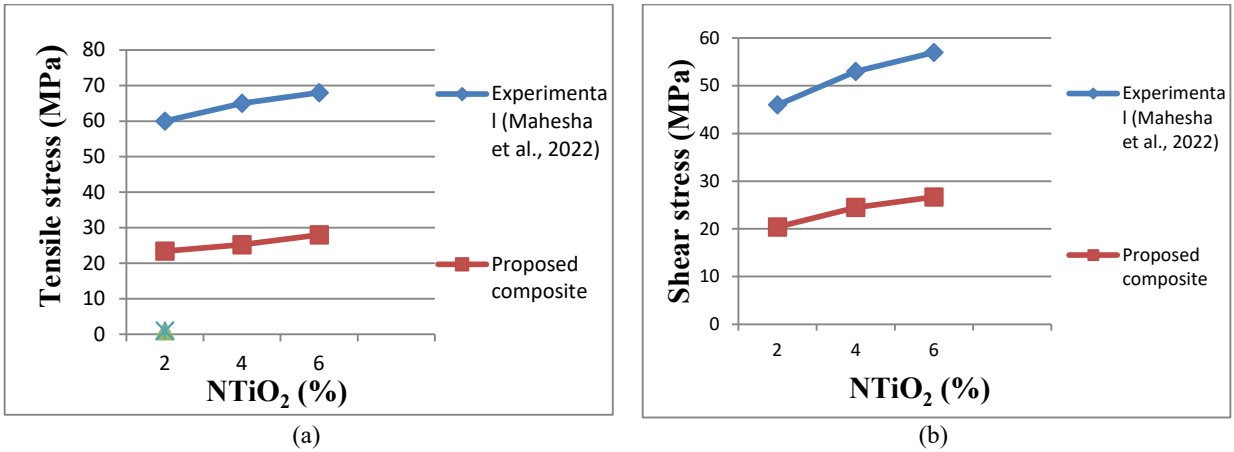

(a) (b)

Fig. 6. Variation of (a) tensile stress and (b) shear stress for (2%, 4% & 6%) weight of $NTiO_2$ filler for the proposed composite values and experimental values (Mahesha et al., 2022).

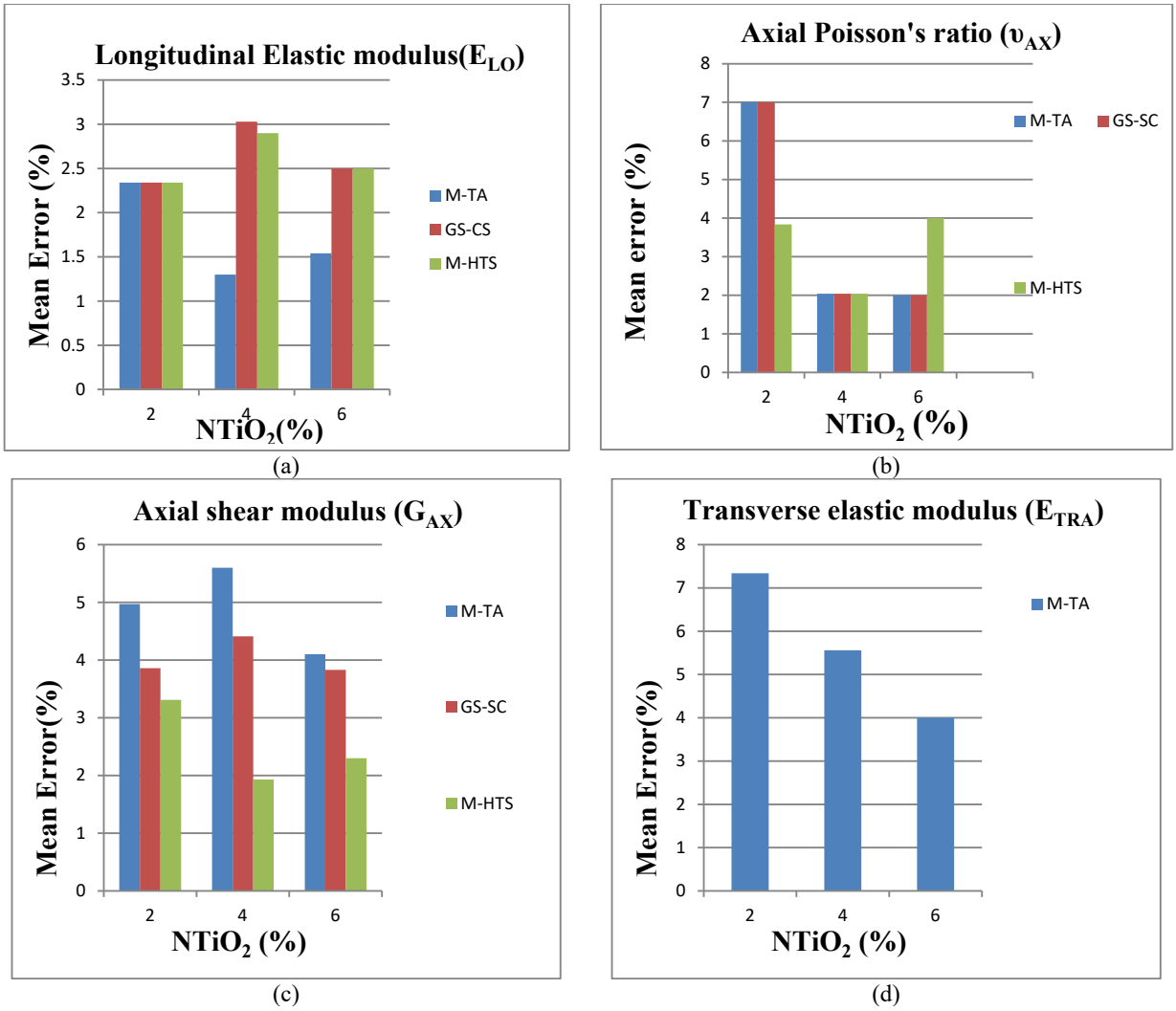

Fig. 7. Results for the mean error for (a) Longitudinal elastic modulus (b) Axial Poisson's ratio (c) Axial shear modulus (d) Transverse elastic modulus

The mean error values are calculated for all the elastic properties obtained from different analytical models for 2%, 4%, and 6% $NTiO_2$ reinforcements and are shown in Fig.7. These errors indicate the percent divergence of the elastic values obtained from analytical models from the elastic values acquired by FEM results. The points given below are summarized from the results shown in Fig. 7.

6.1. Longitudinal elastic modulus (E_{LO})

Longitudinal elastic modulus is the axial stress divided by the uniaxial longitudinal strain that is when there is no strain in the lateral direction. It can be noticed from Fig. 7 (a) that for 6% $NTiO_2$ reinforcement, the M-TA model is showing the least variation from the FEM result, as it is giving the lowest value of the mean error of 1.54% as compared to 2.5% of mean error by GS-C & M-HTS models. For 2%, the mean error % is 2.34 for all the models and shows equal concurrence with FEM results. From the values obtained for E_{LO}, it is found that the proposed composite blended with 6% $NTiO_2$ is more flexible and tough in comparison to 2% & 4% $NTiO_2$ reinforcements.

6.2. Axial Poisson's ratio (υ_{AX})

Axial Poisson's ratio is the degree of transverse elongation of fibers divided by the degree of axial compression of fibers. From Fig. 7(b), it is clear that for 4% $NTiO_2$ reinforcement, the mean error % is 2.04 for all the models and shows equal concurrence and low % variation from FEM results. For 2% $NTiO_2$ reinforcement, both M-TA and GS-C models offer the highest variation of 7.69%, while the M-HTS model yields the lowest variation of 3.84% from FEM results.

6.3. Axial shear modulus (G_{AX})

It is the ratio of shear stress to the specimen's axial displacement per unit length. It is clear from Fig. Fig. 7(d) that for 2%, 4% & 6% reinforcement, M-TA & GS-C models are showing the highest variation in comparison to the results obtained for mean error % for 2%, 4% & 6% $NTiO_2$ reinforcement by M-HTS model.

6.4. Transverse elastic modulus (E_{TRA})

The transverse elastic modulus is the transverse stress divided by the uniaxial transverse strain when no strain exists in the axial direction. It is clear from Fig. 7(c) that the M-TA model for 2% $NTiO_2$ reinforcement yields the highest variation of 7.34% compared to 5.56% and 4.02% for 4% and 6% $NTiO_2$ reinforcement, respectively.

7. Conclusion

A new composite material banana-hemp fiber blended with nano-titanium oxide and an epoxy matrix, is modeled. The composite material developed is examined for elastic properties like longitudinal elastic modulus, transverse elastic modulus, axial Poisson's ratio, and axial shear modulus by using Mori-Tanaka, generalized Self-Consistent, and modified Halpin-Tsai model and validated by FEM results and literature. Total vector sum distortion for 2%, 4%, and 6 weight% of $NTiO_2$ reinforcement in the proposed composite is also calculated. The mean error percent is calculated for all the elastic properties. It shows the deviation from the elastic properties obtained by FEM results. The following points are mentioned:

The elastic properties calculated by the modified Halpin Tsai model for 2%, 4%, and 6 weight% of $NTiO_2$ in the proposed composite are the most effective, as the values obtained by this model show the least mean error percent compared with the FEM results. In contrast, the Mori-Tanaka model is the least efficient as the values obtained by this model show the highest mean error percent.

- The composite reinforced with 6 weight% $NTiO_2$ filler is the most flexible and tough due to its eminent value of longitudinal elastic modulus of 70.2 GPa in contrast to the composite reinforced with 2% and 4 weight% $NTiO_2$ filler.
- Tensile stress in the proposed composite decreases by 61%, and shear stress decreases by 55.6% than in jute-hemp fiber reinforced hybrid composite for 2 wt% nano titanium oxide filler. Adding banana fiber instead of jute fiber in hemp fiber reinforced hybrid composite reduces tensile and shear stress.
- Total vector sum distortion for the arrangement of banana fibers at 45^0, epoxy and $NTiO_2$ particles at $0^{0,}$ and hemp fibers at $45^{0,}$ and for 6 weight% $NTiO_2$ filler composition, is found to be the least, having the value of 0.16208 mm. Therefore, the proposed composite blended with 6 weight% $NTiO_2$ filler has the highest load-carrying capacity and is the strongest among the composites blended with 2% and 4% $NTiO_2$ filler. The composite blended with 2 weight% $NTiO_2$ filler is found to have the lowest strength as this composite is obtained to have the highest total vector sum deformation of 0.16525 mm.
- The hybridization value for the proposed composite is calculated to be 1.5. It shows that the hybrid composite's hemp fiber (high elastic fiber) is 1.5 times tougher than the banana fiber (low elastic fiber) in the hybrid composite. Including banana fiber in the hemp fiber blended composite upgrades the strain rate at which the hybrid composite fails. The hybrid composite has more strength and toughness due to the increase in tensile failure strain features compared to the failure strain of only hemp fiber (HEF fiber) blended composite.

References

Abaimov, S. G., Khudyakova, A. A., & Lomov, S. V. (2016). On the closed-form expression of the Mori–Tanaka theory prediction for the engineering constants of a unidirectional fiber-reinforced ply. *Composite Structures*, *142*, 1-6.

Aliha, M. R. M., Ameri, M., Mansourian, A., & Ayatollahi, M. R. (2012). Finite element analysis of a new test specimen for investigating mixed mode cracks in asphalt overlays. In *7th RILEM International Conference on Cracking in Pavements: Mechanisms, Modeling, Testing, Detection and Prevention Case Histories* (pp. 359-367). Springer Netherlands.

Aliha, M. R. M., Bahmani, A., & Akhondi, S. (2015). Fracture and fatigue analysis for a cracked carabiner using 3D finite element simulations. *Strength of Materials*, *47*, 890-902.

Alvinasab, A. (2009). *Nonlocal theory and finite element modeling of nanocomposites*. Clarkson University.

Benveniste, Y. (1987). A new approach to the application of Mori-Tanaka's theory in composite materials. *Mechanics of materials*, *6*(2), 147-157.

Bhatia, S., Angra, S., & Khan, S. (2021). A review on the mechanical and tribological characterization of boron carbide reinforced epoxy composite. *Advanced Composite Materials*, *30*(4), 307-337.

Budiansky, B. (1965). On the elastic moduli of some heterogeneous materials. *Journal of the Mechanics and Physics of Solids*, *13*(4), 223-227.

Chawla, V. K., Chhabra, D., Gupta, P., & Naaz, S. (2021). Evaluation of green operations management by fuzzy analytical hierarchy process. *Materials Today: Proceedings*, *38*, 274-279.

Chawla, V. K., Itika, Singh, P., & Singh, S. (2023), A fuzzy Pythagorean TODIM method for sustainable ABC analysis in inventory management. *Journal of Future Sustainability, 4(2),* 85-100.

Chawla, V., Bhargava, P., & Verma, S. (2021). Design, stimulation, and fabrication of chassis of an FSAE female driven vehicle. *Materials Today: Proceedings*, *43*, 36-41.

Chou, T. W., Nomura, S., & Taya, M. (1980). A self-consistent approach to the elastic stiffness of short-fiber composites. *Journal of Composite Materials*, *14*(3), 178-188.

Dahlen, C., & Springer, G. S. (1994). Delamination growth in composites under cyclic loads. *Journal of Composite Materials*, *28*(8), 732-781.

DeArmitt, C. (2011). Functional fillers for plastics. In *Applied plastics engineering handbook* (pp. 455-468). William Andrew Publishing.

Dixit, S., & Padhee, S. S. (2019). Finite element analysis of fiber reinforced hybrid composites. *Materials Today: Proceedings*, *18*, 3340-3347.

Essabir, H., Bensalah, M. O., Rodrigue, D., Bouhfid, R., & Qaiss, A. (2016). Structural, mechanical and thermal properties of bio-based hybrid composites from waste coir residues: Fibers and shell particles. *Mechanics of Materials*, *93*, 134-144.

Faghidian, S. A. (2021). Contribution of nonlocal integral elasticity to modified strain gradient theory. *The European Physical Journal Plus*, *136*(5), 559.

Genin, G. M., & Birman, V. (2009). Micromechanics and structural response of functionally graded, particulate-matrix, fiber-reinforced composites. *International journal of solids and structures*, *46*(10), 2136-2150.

Giner, E., Vercher, A., Marco, M., & Arango, C. (2015). Estimation of the reinforcement factor ξ for calculating the transverse stiffness E2 with the Halpin–Tsai equations using the finite element method. *Composite Structures*, *124*, 402-408.

Gupta, P., Chawla, V., Jain, V., & Angra, S. (2022). Green operations management for sustainable development: An explicit analysis by using fuzzy best-worst method. *Decision Science Letters*, *11*(3), 357-366.

Hadden, C. M., Klimek-McDonald, D. R., Pineda, E. J., King, J. A., Reichanadter, A. M., Miskioglu, I., ... & Odegard, G. M. (2015). Mechanical properties of graphene nanoplatelet/carbon fiber/epoxy hybrid composites: Multiscale modeling and experiments. *Carbon*, *95*, 100-112.

Halpin, J. C. (1969). *Effects of Environmental Factors on Composite Materials*. Air Force Materials Lab Wright-Patterson AFB OH.

Hill, R. (1965). A self-consistent mechanics of composite materials. *Journal of the Mechanics and Physics of Solids*, *13*(4), 213-222.

Kobayashi, S., Takada, K., & Nakamura, R. (2014). Processing and characterization of hemp fiber textile composites with micro-braiding technique. *Composites part A: applied science and manufacturing*, *59*, 1-8.

Kumar, A., Angra, S., & Chanda, A. K. (2020). Analysis of the effects of varying core thicknesses of Kevlar Honeycomb sandwich structures under different regimes of testing. *Materials Today: Proceedings*, *21*, 1615-1623.

Kumar, U., Rathi, R., & Sharma, S. (2020). Carbon nano-tube reinforced nylon 6, 6 composites: a molecular dynamics approach. *Engineering Solid Mechanics*, *8*(4), 389-396.

Li, Z., Wang, X., & Wang, L. (2006). Properties of hemp fiber reinforced concrete composites. *Composites part A: applied science and manufacturing*, *37*(3), 497-505.

Mahesha, C. R., Suprabha, R., Harne, M. S., Galme, S. G., Thorat, S. G., Nagabhooshanam, N., ... & Markos, M. (2022). Nanotitanium Oxide Particles and Jute-Hemp Fiber Hybrid Composites: Evaluate the Mechanical, Water Absorptions, and Morphological Behaviors. *Journal of Nanomaterials*, *2022*.

Mori, T., & Tanaka, K. (1973). Average stress in matrix and average elastic energy of materials with misfitting inclusions. *Acta metallurgica*, *21*(5), 571-574.

Ojha, M., Penumakala, P. K., Marrivada, G. V., Chaganti, P. K., & Gupta, A. K. (2019). Processing of glass fiber pultruded composites using graphene nanoplatelets modified epoxy matrix. *Materials Today: Proceedings*, *18*, 3298-3304.

Parashar, S., & Chawla, V. (2023). Kenaf-Coir based hybrid nanocomposite: an analytical and representative volume element analysis. *Engineering Solid Mechanics*, *11*(1), 103-118.

Parashar, S., & Chawla, V. K. (2021). A systematic review on sustainable green fiber reinforced composite and their analytical models. *Materials Today: Proceedings*, *46*, 6541-6546.

Parashar, S., & Chawla, V. K. (2022). Evaluation of fiber volume fraction of kenaf-coir-epoxy based green composite by finite element analysis. *Materials Today: Proceedings*, *50*, 1265-1274.

Parashar, S., & Chawla, V. K. (2022). Evaluation of the effect of Titanium Carbide nanoparticles reinforcement in Kenaf Coir fibre-based Epoxy Hybrid Composites. *Neuroquantology, 20*(10), 3922-3933.

Parashar, S., & Tomar, P. (2019, February). Synergy of sustainable bio-composite bamboo material in green technology–an explicit report. In *Proceedings of International Conference on Sustainable Computing in Science, Technology, and Management (SUSCOM), Amity University Rajasthan, Jaipur-India*.

Parashar, S., & Chawla, V.K. (2023). Analysis of the Effect of Hybridization of Coconut Shell Particles on Kenaf-Coir Based Epoxy Hybrid Composites. *Energy and Environment Focus*, *7*(1), 65-76.

Perreault, F., De Faria, A. F., & Elimelech, M. (2015). Environmental applications of graphene-based nanomaterials. *Chemical Society Reviews*, *44*(16), 5861-5896.

Pol, A., Malagi, R., & Munshi, G. (2022). Identification of mechanical properties of an araldite LY556 blended with DNR composite and polyacetal: A comparative study for sustainable future. *Journal of Future Sustainability*, *2*(4), 149-156.

Rafiee, M., Nitzsche, F., & Labrosse, M. R. (2018). Modeling and mechanical analysis of multiscale fiber-reinforced graphene composites: Nonlinear bending, thermal post-buckling, and large amplitude vibration. *International Journal of Non-Linear Mechanics*, *103*, 104-112.

Raghavendra, G., Ojha, S., Acharya, S. K., & Pal, S. K. (2015). Influence of micro/nanofiller alumina on the mechanical behavior of novel hybrid epoxy nanocomposites. *High Performance Polymers*, *27*(3), 342-351.

Ramakrishna, S., Lim, T. C., Inai, R., & Fujihara, K. (2006). Modified Halpin-Tsai equation for clay-reinforced polymer nanofiber. *Mechanics of Advanced Materials and Structures*, *13*(1), 77-81.

Sadjadi, S. (2021). A survey on the effect of plastic pollution in the Great Lakes. *Journal of Future Sustainability*, *1*(1), 5-8.

Sadjadi, S. S., & Ghaderi, S. F. (2023). The role of interest rate and inflation on oil stock prices: Evidence from Ukraine-Russia war. *Journal of Industrial and Systems Engineering*, (Articles in Press).

Sapuan, S. M., Leenie, A., Harimi, M., & Beng, Y. K. (2006). Mechanical properties of woven banana fibre reinforced epoxy composites. *Materials & design*, *27*(8), 689-693.

Saxena, A., Dwivedi, S. P., Dixit, A., Sharma, S., Srivastava, A. K., & Maurya, N. K. (2021). Computational and experimental investigation on mechanical behavior of zirconia toughened alumina and nickel powder reinforced EN31 based composite material. *Materialwissenschaft und Werkstofftechnik*, *52*(5), 548-560.

Saxena, T., & Chawla, V. K. (2021). Banana leaf fiber-based green composite: An explicit review report. *Materials Today: Proceedings*, *46*, 6618-6624.

Saxena, T., & Chawla, V. K. (2022). Effect of fiber orientations and their weight percentage on banana fiber-based hybrid composite. *Materials Today: Proceedings*, *50*, 1275-1281.

Saxena, T., & Chawla, V. K. (2022). Evaluation of mechanical properties for banana-carbon fiber reinforced nano-clay epoxy composite using analytical modeling and simulation. *Research on Engineering Structures and Materials, 8(*4), 773-798.

Saxena, T., & Tomar, P. (2019, February). Constitutive Performance Characterization of Diversified Bamboo Material–A Green Technology. In *Proceedings of International Conference on Sustainable Computing in Science, Technology and Management (SUSCOM), Amity University Rajasthan, Jaipur-India*.

Seretis, G. V., Kouzilos, G., Manolakos, D. E., & Provatidis, C. G. (2017). On the graphene nanoplatelets reinforcement of hand lay-up glass fabric/epoxy laminated composites. *Composites Part B: Engineering*, *118*, 26-32.

Seshanandan, G., Ravindran, D., & Sornakumar, T. (2016). Mechanical properties of nano titanium oxide particles-hybrid jute-glass FRP composites. *Materials Today: Proceedings*, *3*(6), 1383-1388.

Singh, S., & Angra, S. (2018). Flexural and impact properties of stainless steel based glass fibre reinforced fibre metal laminate under hygrothermal conditioning. *International Journal of Engineering*, *31*(1), 164-172.

Tekletsadik, S. (2023). Selection of best leather item using a FAHP method to launch new leather industry in Ethiopia: A case study. *Journal of Future Sustainability*, *3*(2), 85-96.

Thwe, M. M., & Liao, K. (2002). Effects of environmental aging on the mechanical properties of bamboo–glass fiber reinforced polymer matrix hybrid composites. *Composites Part A: Applied Science and Manufacturing*, *33*(1), 43-52.

Tsai, S. W., & Hahn, H. T. (2018). *Introduction to composite materials*. Routledge.

Van Loan, C. F., & Golub, G. (1996). Matrix computations (Johns Hopkins studies in mathematical sciences). *Matrix Computations*, *53*.

Wang, H. (2002). *Design and optimisation of chemical and mechanical processing of hemp for rotor spinning and textile applications* (Doctoral dissertation, UNSW Sydney).

Wang, H. M., Postle, R., Kessler, R. W., & Kessler, W. (2001). Adaptive processing of Australia hemp for short fibre spinning. *Bast fibrous plants on the turn of second and third millennium, Shenyang, China*.

Wang, Y., & Huang, Z. (2017). A review of analytical micromechanics models on composite elastoplastic behaviour. *Procedia engineering*, *173*, 1283-1290.

Yadav, E., & Chawla, V. K. (2022). An explicit literature review on bearing materials and their defect detection techniques. *Materials Today: Proceedings*, *50*, 1637-1643.

Younes, R., Hallal, A., Fardoun, F., & Chehade, F. H. (2012). Comparative review study on elastic properties modeling for unidirectional composite materials. *Composites and their properties*, *17*, 391-408.

Yung, K. C., Wang, J., & Yue, T. M. (2006). Modeling Young's modulus of polymer-layered silicate nanocomposites using a modified Halpin—Tsai micromechanical model. *Journal of reinforced plastics and composites*, *25*(8), 847-861.

Zweben, C. (1977). Tensile strength of hybrid composites. *Journal of materials science*, *12*, 1325-1337.